

Self-Assembly of *n*-Alkanethiolate Monolayers on Silver Nanostructures: Protective Encapsulation

Wenjie Li, J. A. Virtanen, and R. M. Penner*

Institute for Surface and Interface Science (ISIS), Department of Chemistry, University of California, Irvine, Irvine, California 92717-2025

Received November 29, 1994. In Final Form: February 21, 1995[⊗]

Electrochemically synthesized silver nanostructures having dimensions 200–1000 Å in diameter and 20–50 Å high were prepared on graphite surfaces using the scanning tunneling microscope (STM). These nanostructures were stable while immersed in aqueous solutions containing small (0.5 mM) concentrations of Ag⁺ during repeated STM imaging at small sample-negative biases for at least 1 h. Upon exchange of the silver plating solution for pure water, dissolution of the nanostructure occurred within 30 min, irrespective of the applied imaging bias up to ±200 mV. The anodic dissolution of silver nanostructures in pure water was strongly inhibited following the formation of an *n*-alkanethiolate self-assembled monolayer (SAM) on the silver surface, demonstrating that molecular self-assembly provides a method for the protective, and chemically selective, encapsulation of reactive nanometer-scale structures on solid surfaces. In contrast, self-assembly was not observed following the exposure of silver nanostructures to long-chain *n*-alkylamines or carboxylic acids and these prospective ligands provided no protection from dissolution of the nanostructure in pure water.

Introduction

Recently, the scanning tunneling microscope (STM) has been employed to electrochemically deposit nanoscopic silver and copper disk-shaped structures having typical dimensions of 200–500 Å in diameter and 20–100 Å in height on graphite basal plane surfaces.^{1–4} Metal deposition occurs via a two-step mechanism in which a shallow pit in the graphite surface is first formed⁵ followed immediately by electrochemical deposition of metal at this nucleation site.¹ The metal nanostructures prepared by this procedure are ideal candidates for investigations of stability and corrosion using *in situ* STM imaging in part because these nanostructures are strongly anchored to the graphite surface and are immobile during repeated STM imaging.^{1–4} In addition, each metal nanostructure protrudes from an atomically smooth graphite surface which is electrochemically unreactive. The graphite surface functions as a baseline against which small changes in the height of a metal nanostructure—resulting either from electrochemical reactions of the metal nanostructures³ or from the adsorption of molecules from solution²—can be accurately measured. For example, we have previously demonstrated that the time dependence of the nanostructure height (measured with the STM in an aqueous solution) can be used to track the spontaneous electrochemical reactions of coexisting copper and silver nanostructures on graphite.³

Here we report the results of experiments in which the stability of silver nanodisk structures in dilute silver-ion-containing solutions and in pure water is compared. An important conclusion of this study is that in aqueous solution, silver nanostructures are inherently unstable in the absence of small concentrations (e.g. 0.5 mM) of silver ions. The observed instability of silver nanostructures

provides a serious barrier to the preparation by electrochemical deposition of ensemble surface nanostructures composed of metals (or other materials) other than silver. Consequently, we have sought a method by which metal nanostructures might be stabilized in aqueous solutions in which ions of the metal are not present.

We have very recently reported² the results of experiments in which an *n*-alkanethiolate layer is self-assembled on the surface of silver nanodisk structures which were electrochemically deposited on graphite surfaces using our procedure. In this previous work, the thickness of the *n*-alkanethiolate monolayer was compared with the expected monolayer thickness based on two structural models for the monolayer.² Previously, *n*-alkanethiolate self-assembled monolayers (SAMs) have been employed as passivating layers for gold, silver, and copper surfaces exposed to air and solution.^{6–18} Here we report that *n*-alkanethiolate SAMs perform this same function at nanoscopic silver surfaces: Whereas silver nanostructures spontaneously dissolve in a deionized water ambient, following self-assembly of an *n*-alkanethiolate monolayer on a silver nanostructure, no erosion in the height (or volume¹⁹) of the structure was detected during exposures to deionized water of up to 1 h. Other prospective ligands including two long-chain *n*-alkylamines and a long-chain *n*-alkylcarboxylic acid were not observed to self-assemble at the silver surface. Exposure of silver nanostructures

(6) Chidsey, C. E. D.; Loiacono, D. N. *Langmuir* **1990**, *6*, 682.

(7) Chidsey, C. E. D. *Science* **1991**, *251*, 919.

(8) Finklea, H. O.; Robinson, L. R.; Blackburn, A.; Richter, B.; Allara, D.; Bright, T. *Langmuir* **1986**, *2*, 239.

(9) Finklea, H. O.; Avery, S.; Lynch, M.; Furtch, T. *Langmuir* **1987**, *3*, 409.

(10) Kumar, A.; Biebuyck, H. A.; Abbott, N. L.; Whitesides, G. M. *J. Am. Chem. Soc.* **1992**, *114*, 9188.

(11) Kumar, A.; Whitesides, G. M. *Appl. Phys. Lett.* **1993**, *63*, 2002.

(12) Kumar, A.; Whitesides, G. M. *Science* **1994**, *263*, 60.

(13) Laibinis, P. E.; Whitesides, G. M. *J. Am. Chem. Soc.* **1992**, *114*, 9022.

(14) Porter, M. D.; Bright, T. B.; Allara, D. L.; Chidsey, C. E. D. *J. Am. Chem. Soc.* **1987**, *109*, 3559.

(15) Rubinstein, I.; Steinberg, S.; Tor, Y.; Shanzer, A.; Sagiv, J. *Nature* **1988**, *332*, 426.

(16) Sabatini, E.; Rubinstein, I.; Maoz, R.; Sagiv, J. *J. Electroanal. Chem.* **1987**, *219*, 365.

(17) Sabatini, E.; Rubinstein, I. *J. Phys. Chem.* **1987**, *91*, 6663.

(18) Sun, L.; Crooks, R. M. *Langmuir* **1993**, *9*, 1951.

* Address correspondence to this author at: RMPenner@UCI.edu.

⊗ Abstract published in *Advance ACS Abstracts*, October 1, 1995.

(1) Li, W.; Duong, T.; Virtanen, J. A.; Penner, R. M. *Proc. NATO ASI*, in press.

(2) Li, W.; Virtanen, J. A.; Penner, R. M. *J. Phys. Chem.* **1994**, *98*, 11751.

(3) Li, W.; Virtanen, J. A.; Penner, R. M. *Appl. Phys. Lett.* **1992**, *60*, 1181.

(4) Li, W.; Virtanen, J. A.; Penner, R. M. *J. Phys. Chem.* **1992**, *96*, 6529.

(5) Penner, R. M.; Heben, M. J.; Lewis, N. S.; Quate, C. F. *Appl. Phys. Lett.* **1991**, *58*, 1389.

to these other ligands coincided with the onset of nanostructure height instability and rapid dissolution.

Experimental Section

STM imaging experiments were conducted using a modified Park Scientific Instruments AutoProbe cp STM/AFM in the conventional two electrode (i.e. tip and sample) mode. A Kel-F electrochemical sample holder permitted the exposure of a 6 mm diameter circular region of a graphite surface to a solution volume of 200 μL . Flexible Tygon tubing and a 20 mL syringe were employed to replace the AgF-containing plating solution with pure water during STM imaging investigations of silver nanostructure stability. STM tips were constructed from electrochemically etched 0.5 mm diameter platinum wire which was coated with poly- α -methylstyrene polymer as previously described.²⁰ The output from an arbitrary waveform generator (Stanford Model DS340) was added to the sample potential in order to effect silver nanostructure deposition as described below.

Silver nanodisks were grown electrochemically on graphite surfaces using previously described procedures.^{1,3,4} Briefly, electrochemical growth of silver nanostructures was induced by the application of 6.0 V \times 50 μs (tip-positive) bias voltage pulses from the arbitrary waveform generator between the STM tip and a graphite surface immersed in aqueous 0.5 mM AgF (Aldrich, >99.99%). The bias pulse induced the electrochemical growth of a nanoscopic silver adsorption site by a two-step mechanism involving the formation of a monolayer-deep pit in the graphite surface within 5 μs of the application of the bias pulse and the subsequent diffusion-controlled deposition of silver until the termination of the pulse at 50 μsec .¹

Following the deposition and *in situ* characterization of the deposit by STM imaging, the ligand of interest was introduced into the STM using either of two methods: For liquids ($n \leq 16$), 20 μL of neat ligand was injected into the 200 μL of the aqueous 0.5 mM silver plating solution contained in the Kel-F sample holder in the STM. Following injection, approximately 5 min elapsed before high magnification STM images of the nanostructure could be reacquired. Alternatively, *n*-octadecanethiol—a solid at room temperature—was introduced as a solution in *n*-octane using the same technique. Following introduction into the STM electrochemical cell, this *n*-octane solution floated as a thin film on the surface of the aqueous electrolyte in the cell, and partitioning of the *n*-alkanethiol into the electrolyte occurred.

Results and Discussion

In situ STM imaging is one method by which the stability of immobilized metal particles may be investigated. The silver nanostructures prepared using the method outlined above are particularly attractive candidates for these investigations since—as previously demonstrated^{1–4}—these particles are anchored to the graphite substrate surface at defect sites and are immobile during repeated STM imaging in aqueous solutions. In a previous paper, we demonstrated that either silver or copper nanostructures are stable when imaged in dilute solutions of their respective ions at tip–sample biases which are small (20–40 mV) and tip-positive.⁴ For the silver nanostructures which are the subject of this paper, this fact is confirmed in the experiment of Figure 1. Figure 1A shows STM images of a silver nanostructure synthesized using a single

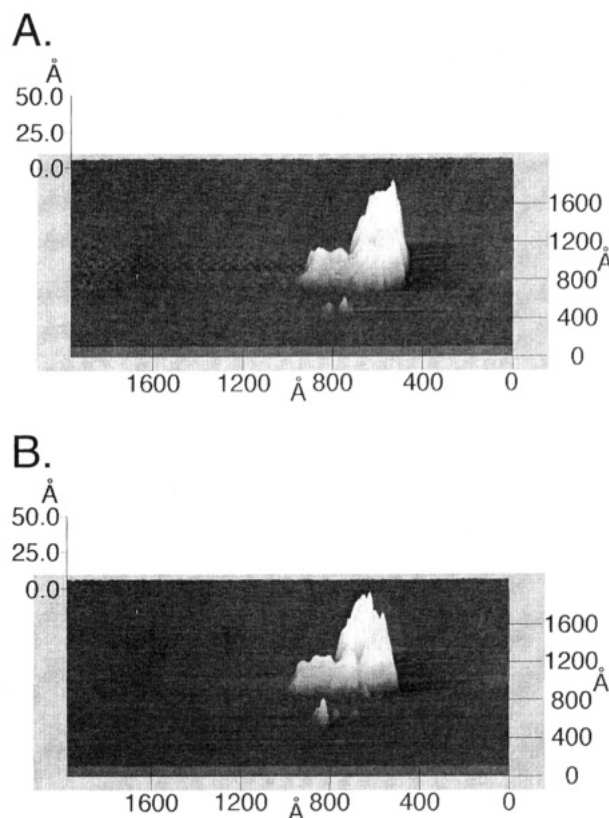


Figure 1. STM images of a silver nanostructure electrochemically deposited on a graphite surface: (A) The silver nanostructure is shown immediately following deposition in an aqueous solution of 0.5 mM AgF. (B) The same silver nanostructure is shown following 32 min and the acquisition of 20 STM images. Both images were acquired using an imaging bias of $E_B = 24$ mV (tip positive) and a tunneling current of $i_t = 0.8$ nA.

–6.0 V \times 50 μs bias pulse. This nanostructure possessed an unusually distinctive and complicated shape which increases the likelihood that either small additions or subtractions of silver resulting from electrochemical reactions will be observable in STM images. The same particle is shown 32 min later in Figure 1B following the acquisition of 20 STM images using an imaging bias of +24 mV (tip vs sample) and a set-point current of 0.8 nA. No changes in the height or the apparent volume of the nanostructure were observed within the reproducibility of this measurement of approximately ± 5 Å in height and ± 200 Å³ in volume.

This stability observed during STM imaging at sample-negative biases is not retained for tip-negative biases of 20–40 mV.¹ In this case, dissolution of silver nanostructures is usually observed. In other words, a change of the imaging bias of 40 mV (from +20 to –20 mV) induces a transition to instability from stability for silver nanostructures immersed in 0.5 mM AgF. This observation suggests that the open-circuit potential of the graphite surface in these experiments is within 40 mV of the Nernst potential for silver when the surface is in contact with a dilute aqueous Ag⁺-containing solution although only a few nanostructures are present on the graphite surface.¹ In fact, the potential of the graphite surface with attached silver nanostructures can be directly measured versus a silver wire using a high impedance voltmeter, and this potential is typically within 5 mV of a silver wire reference immersed in the same aqueous, 0.5 mM AgF solution. The effect of an applied imaging bias of ± 20 mV is therefore to displace the graphite surface potential either in the direction of anodic dissolution or in the direction of silver metal deposition; however the rate of the resulting cathodic

(19) It is widely appreciated that the volume of a protrusion on a surface, estimated by integrating STM line scans, actually provides an upper limit to the volume. The apparent nanostructure volume obtained by this method equals the true nanostructure volume only in the limit of an infinitely sharp STM tip and an infinitely high density of STM line scans (in the slow scan direction of STM image acquisition). The effect of finite STM tip size is to exaggerate the dimensions of protrusions on a surface and in the limit of an infinitely sharp protrusion on an atomically smooth surface, the apparent nanostructure geometry matches that of the STM tip. Conclusions based on absolute nanostructure volumes are therefore potentially misleading, and in this work, conclusions are derived only from changes in the nanostructure volume and geometry which are observed with time. These conclusions are subject to the assumption that the geometry of the platinum STM tip is invariant over the duration of the experiment.

(20) Penner, R. M.; Heben, M. J.; Lewis, N. S. *Anal. Chem.* **1989**, *61*, 1630.

polarization is clearly not appreciable (because in experiments like that shown in Figure 1, no increase in the nanostructure dimension is detected). The tip-sample imaging bias therefore provides control over the nanostructure stability even in the simplest two-electrode *in situ* STM imaging configuration.

It is important to recognize that the Nernst potential for silver nanostructures will only be defined in the presence of silver ion in the contacting aqueous solution. When the silver ion-containing solution is replaced with pure water, silver dissolution commences and the dimensions of silver nanostructures become smaller with time. In Figure 2A, for example, a silver nanostructure having a height of 65 Å is shown immediately following electrochemical deposition in aqueous 0.5 mM AgF. Following exchange of the 0.5 mM AgF plating solution for pure water, the STM images shown in parts B and C of Figure 2, taken at intervals of 6 and 30 min after exchange, show an obvious decrease in height. A plot of the average height versus time shown in Figure 2D reveals a decrease from 64 to 26 Å over the course of 30 min following the introduction of pure water to the cell. The dissolution of metal nanodots is reproducibly observed upon exposure to pure water for nanostructures of cadmium and copper as well as silver at imaging biases of 30 mV. This instability is due to the positive drift of the electrochemical potential of the surface from the reversible Nernst potential for the metal and its ions, because the Nernst potential of the surface is undefined in pure water. This potential drift of the surface relative to a reference electrode is experimentally measurable, and it is not eliminated by increasing the STM imaging bias voltage to values as high as +200 mV.

Previously we have shown that if instead of pure water, aqueous 0.5 mM Cu²⁺ is substituted for the silver plating solution and copper nanostructures are deposited, a spontaneous electrochemical reaction occurs in which a few monolayers of copper plate onto the silver nanostructures.³ Designed nanometer-scale electrochemical reactions such as this galvanic discharge have many potential applications; however, electrochemical "cross-talk" of this type can also be undesirable during electrochemical nanofabrication since contamination of nanostructures can occur.

A well-known strategy for protecting metal surfaces from corrosion is to apply a coating which blocks electronic and ionic conduction to a contacting aqueous phase and restricts access of uncharged reactants such as water and O₂ to the metal surface. Previously it has been demonstrated that for macroscopic surfaces of copper¹³ and gold,^{6,9,14,15,17,21,22} a single self-assembled monolayer (SAM) of *n*-alkanethiol molecules effectively accomplishes one or more of these functions provided the alkyl chain length of the thiols is approximately C₈ or greater. In the context of electrochemical nanofabrication experiments on graphite surfaces, *n*-alkanethiolate monolayers are expected to spontaneously and selectively assemble at nanostructures composed of silver, copper, and gold, but not at the graphite surface which is inert to thiol chemisorption. For silver nanostructures, this expectation is confirmed by the data of Figure 3: An STM image of two silver nanostructures immersed in the aqueous 0.5 mM AgF solution from which they were deposited is shown in Figure 3A. The cross sections shown in Figure 3D reveal the diameters of these structures are approximately 500 and 300 Å, respectively. The nanostructure dimensions apparent in Figure 3D were stable to within ±5% for a period of approximately 30 min during repetitive STM imaging in this solution at an

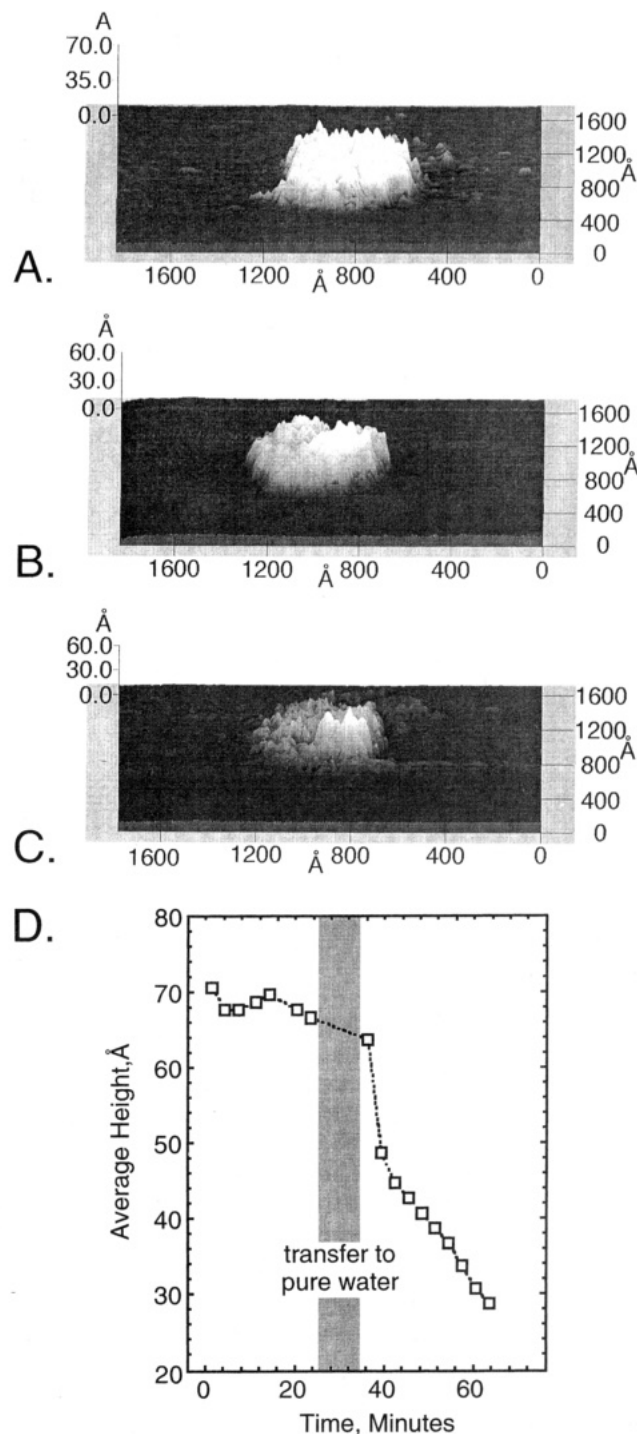


Figure 2. STM images of a silver nanostructure electrochemically deposited on a graphite surface: (A) The silver nanostructure is shown immediately following deposition in an aqueous solution of 0.5 mM AgF. Deposition was effected by the application of a single, tip-positive bias pulse of $6 \text{ V} \times 50 \mu\text{s}$ between the STM tip and the graphite surface in this solution. The same nanostructure is shown (B) immediately (i.e., within 1 min) following the exchange of the silver plating solution for pure water solution and (C) after 5 min in pure water. All images were acquired using an imaging bias of $E_B = 30 \text{ mV}$ (tip positive) and a tunneling current of $i_t = 0.6 \text{ nA}$. (D) Plot of the average height of the silver nanostructure shown in Figure 2 versus time showing the monotonic deterioration of the nanostructure height.

applied bias of +24 mV. In Figure 3B, the same nanostructures are shown following exposure to an aqueous solution saturated with dodecanethiol ($\text{CH}_3(\text{CH}_2)_{11}\text{SH}$), exchange of plating solution for pure water, and exposure to pure water for 10 min during the acquisition of nine STM images. The cross section shown in Figure 3C

(21) Steinberg, S.; Rubinstein, I. *Langmuir* **1992**, *8*, 1183.

(22) Chailapakul, O.; Sun, L.; Xu, C.; Crooks, R. M. *J. Am. Chem. Soc.* **1993**, *115*, 12459.

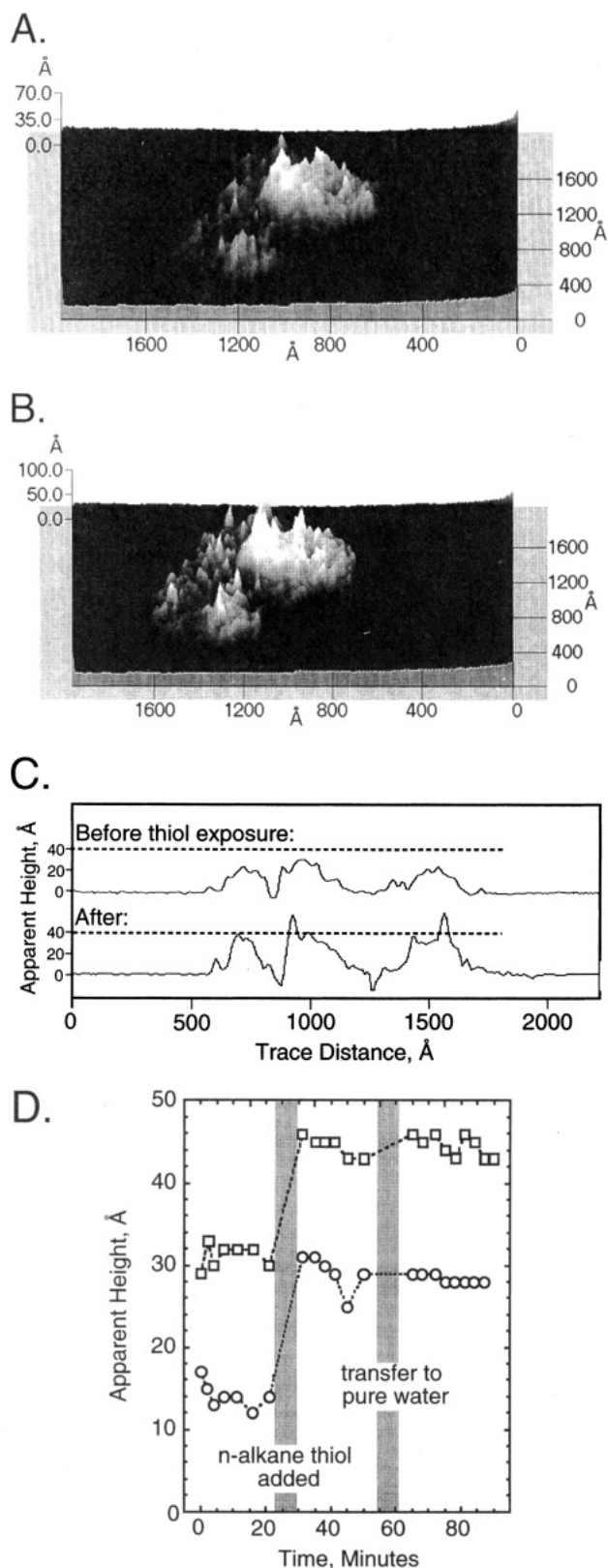


Figure 3. STM images of two silver nanostructures electrochemically deposited on a graphite surface: (A) The silver nanostructures are shown immediately following deposition in an aqueous solution of 0.5 mM AgF. (B) The same nanostructures are shown following the addition of *n*-dodecanethiol to this solution, exchange of this thiol-containing plating solution for pure water, and exposure to the pure water ambient for 20 min. All images were acquired using an imaging bias of $E_B = 30$ mV (tip positive) and a tunneling current of $i_t = 0.6$ nA. (C) Cross sections for the nanostructures shown in A (labeled before) and B (labeled after) are shown. (D) Plot of the average heights of both nanostructures as a function of time during the exposure of these nanostructures to dodecanethiol and exchange of this thiol-containing plating solution for pure water.

(marked "after") shows that in contrast to the deterioration in height normally observed following exposure to pure water, the maximum heights of both nanostructures have increased to near 40 Å.

Recently, we have reported that for a series of *n*-alkanethiols varying in length from C₁₀ (all-trans length 16 Å) to C₁₈ (26 Å), the stepwise height increase observed for silver nanostructures following thiol exposure increases linearly with the *n*-alkyl chain length.² For the longest members of this series (C₁₆ and C₁₈) which are well below their respective chain melting transition temperatures at room temperature, the observed height increment approximately equals the expected all-trans chain length for these thiols indicating that little STM tip penetration into the thiolate layer occurs during imaging. This result was obtained using tunneling currents of 0.2–0.8 nA and tip-positive imaging biases of 40 mV corresponding to a tunneling gap resistance in the interval from 50 to 200 MΩ. The height increases observed for the two nanostructures shown in Figure 3 are approximately 15 Å following exposure to dodecanethiol (all-trans length = 18.7 Å), which is consistent with our previously reported results.²

Following thiol exposure and SAM formation, the thiol-containing electrolyte was replaced with deionized water. A plot of the nanostructure height versus time shown in Figure 3D shows that no detectible dissolution of the nanostructure occurs for the ensuing 30 min exposure to water (and for an additional 30 min which are not plotted in Figure 3D). The apparent stability in water of the nanostructures shown in Figure 3 is attributed to the insulation of the silver surface from ions and solvent by the *n*-alkanethiolate SAM. The stabilization of silver nanostructures in pure water was observed following the exposure of silver nanostructures to any of five different *n*-alkanethiols having alkyl chain lengths of C₁₀, C₁₂, C₁₄, C₁₆, and C₁₈. These experiments demonstrate silver nanostructures may be protected from dissolution by encapsulation in a protective *n*-alkanethiolate SAM.

Although it is likely that the SAM imposes a physical barrier to ion transport with dissolved species in solution, the *n*-alkanethiolate monolayer may also modify the reactivity of silver nanostructures via an electronic mechanism. Chemisorption of a nucleophilic thiol molecule on silver is accompanied by charge donation to the metal. The cumulative effect of the adsorption of many thiol molecules is a negative shift of the Fermi level which is predicted to be appreciable (e.g., 0.40 eV²³) for silver colloids having diameters of a few angstroms. Henglein and co-workers^{23,24} have recently invoked this mechanism to account for the increased reactivity of silver colloids toward dissolved O₂ and changes in the absorption spectrum for these colloids, following exposure to SH⁻. For the much larger silver nanostructures which are the topic of the present work, the magnitude of the negative shift of the Fermi energy brought about by electron donation from adsorbed thiols is 20 meV.²⁵ The significance of this electronic mechanism to the stabilization of silver nanostructures should be elucidated by experiments in which the stabilizing influence of short chain thiols is measured. For these thinner monolayers, the electronic contribution to stabilization conferred by the thiolate is present; however the physical barrier to charge transport should be substantially smaller. These investigations are currently in progress.

In addition to thiols, other ligands which complex silver ions may be strongly adsorbed at silver nanostructures,

(23) Mulvaney, P.; Linnert, T.; Henglein, A. *J. Phys. Chem.* **1991**, *95*, 7843.

(24) Henglein, A.; Linnert, T.; Mulvaney, P. *Ber. Bunsenges. Phys. Chem.* **1990**, *94*, 1449.

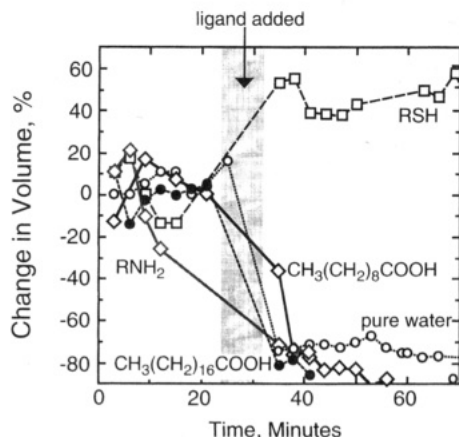


Figure 4. Plots of the average height of five different nanostructures following exposure to various ligands and deionized water: solid circle, $\text{CH}_3(\text{CH}_2)_{16}\text{COOH}$; open box, $\text{CH}_3(\text{CH}_2)_{17}\text{SH}$; open diamond, $\text{CH}_3(\text{CH}_2)_8\text{COOH}$; gray open diamond, $\text{CH}_3(\text{CH}_2)_{17}\text{NH}_2$; open circle, deionized water.

and these ligands also have the potential to modify reactivity. Two other candidates are *n*-alkylamines and carboxylic acids. Figure 4 shows the effect on the silver nanostructure height of the addition of C_{10} and C_{18} *n*-alkylcarboxylic acids and a C_{18} amine to the pH 6.0 aqueous 0.5 mM AgF solution employed for deposition. Also shown for purposes of comparison are representative experiments involving water exposure in the absence of

(25) In the context of a free-electron gas approximation, the Fermi energy, ϵ_F , of a metal nanostructure is related to the nanostructure volume, V , and the total number of electrons, N , by²⁶

$$\epsilon_F = \frac{\hbar^2}{2m} \left(3\pi^2 \frac{N}{V} \right)^{2/3} \quad (\text{i})$$

where m is the electron mass. An increase of N by a small fraction, x , results in a change of the Fermi energy given by

$$\Delta\epsilon_F = \frac{2}{3} \epsilon_F x \quad (\text{ii})$$

The fraction, x , can be estimated as the product of three terms: the fraction of the total number of atoms in a nanostructure (N) which are surface atoms (n_s), the fraction of surface atoms on which are bonded an alkanethiolate adsorbate, and the fractional charge associated with each chemisorption bond, δe . Assuming that the $(\sqrt{3} \times \sqrt{3})R30^\circ$ ordering of alkanethiolate molecules on $\text{Au}(111)$ ^{28,29} approximately obtains for the silver nanostructures investigated here, $1/3$ of all surface atoms are directly bonded to a thiol molecule. x is therefore given by²⁷

$$x = \frac{1}{3} \frac{n_s}{N} \delta \quad (\text{iii})$$

and $\Delta\epsilon_F$ is

$$\Delta\epsilon_F = \frac{2}{9} \epsilon_F \frac{n_s}{N} \delta \quad (\text{iv})$$

For a disk-shaped silver nanostructure having typical dimensions of 500 Å in diameter and 50 Å in height (as shown, for example in Figure 2), the surface area and volume are $2.75 \times 10^5 \text{ Å}^2$ (or $2.75 \times 10^{-11} \text{ cm}^2$) and $9.8 \times 10^6 \text{ Å}^3$ (or $9.8 \times 10^{-18} \text{ cm}^3$) corresponding to $n_s = 3.1 \times 10^4$ silver atoms and $N = 5.8 \times 10^5$ silver atoms, respectively. If ϵ_F and δ are taken to be 5.48 eV²⁷ and 0.3, respectively, eq iv yields a negative shift of 20 meV.

a ligand and *n*-alkanethiolate exposure for *n*-octadecanethiolate. Only following exposure to *n*-octadecanethiol is an increase in the nanostructure height observed as a consequence of monolayer self-assembly. Exposure to either of the carboxylic acids or the amine coincided with an immediate onset of height instability and the eventual dissolution of the nanostructure in 20–40 min. As shown in the plots of Figure 4, this instability mimics the behavior observed for unprotected silver nanostructures exposed to pure water. On the basis of this similarity, it is likely that this ligand-induced instability derives from the lowering of the free silver ion concentration in solution caused by the formation of soluble silver complexes.

Summary

The protective encapsulation of silver nanostructures by self-assembled monolayers of *n*-alkanethiols has been demonstrated. For unmodified silver nanostructures having typical dimensions of 200–1000 Å in diameter and 20–50 Å in height, nanostructure dimensions are unaffected by STM imaging at modest, sample-negative biases of 20–40 mV in dilute silver-ion-containing solutions having $[\text{Ag}^+] 0.5 \text{ mM}$. Replacement of the silver electrolyte with pure water, however, causes an immediate onset of instability and the rapid dissolution of the nanostructure within 30 min—irrespective of the applied imaging bias up to +200 mV.

The exposure of graphite-supported silver nanostructures to aqueous solutions of *n*-alkanethiolates results in the spontaneous self-assembly of monolayers on these structures. Following thiol exposure, SAM formation is immediately apparent as a stepwise increase in the nanostructure height as previously described.² Following SAM formation, the dissolution of silver nanostructures following exposure to pure is strongly inhibited for durations of exposure of up to 1 h. The nanostructure capping strategy demonstrated here is expected to afford new flexibility in the preparation of ensembles of nanostructures composed of different materials using a variety of synthetic methods.

Acknowledgment. The financial support of this research by the Office of Naval Research (400XYIP119) and the National Science Foundation (DMR-9257000) is gratefully acknowledged. R.M.P. also acknowledges financial support in connection with an Alfred P. Sloan Research Fellowship. The authors thank Mr. Art Moore of Advanced Ceramics, Inc., for donations of highly oriented pyrolytic graphite employed in these experiments. J.A.V. thanks the Finnish Cultural Foundation for financial assistance.

LA9409440

(26) Kittel, C. *Introduction to Solid State Physics*, 6th ed.; John Wiley & Sons: New York, 1986.

(27) Henglein, A. *J. Phys. Chem.* **1993**, *97*,

(28) Chidsey, C. E. D.; Liu, G. Y.; Rowntree, P.; Scoles, G. *J. Chem. Phys.* **1989**, *91*, 4421.

(29) Strong, L.; Whitesides, G. M. *Langmuir* **1988**, *4*, 546.